AIAA JOURNAL
Vol. 33, No. 9, September 1995

Whirl Speeds and Stability of Rotating Shaft Subjected to End Loads

Lien-Wen Chen* and Hwang-Kuen Chen†
National Cheng Kung University, Tainan 70101, Taiwan, Republic of China

The variation of natural whirl speeds and instability of a rotating shaft subjected to end loads (i.e., axial compressive forces, moments, and torques) are studied. A finite element model of a Timoshenko beam is adopted to approximate the continuous shaft, and important factors such as the rotatory inertia, shear deformations, and gyroscopic moments are taken into account. The results show that the natural whirl speeds of the shaft do not always decrease when the loads increase and the types of system instability resulting from different end loads are not the same.

I. Introduction

SINCE the first published work of Rankine[1] in 1869, many researchers have devoted themselves to investigating the behavior of rotor systems under various operating situations. Because of the necessity of saving weight and the requirement of acquiring higher performance in the design of rotor systems, accurate predictions of vibrational characteristics and stability analyses of the systems have become increasingly important. In the past, many research workers had focused attention on the dynamic instability of rotor systems caused by self-excited or inherent instability factors, and a number of destabilizing mechanisms such as the fluid film in bearings, fluid ring seals, and the internal friction in rotating parts had been identified or hypothesized to explain the occurrence of unstable phenomena. Some known sources of destabilizing forces in turbomachinery are classified and listed in Ref. 2.

Rotordynamic characteristics may also change when the rotor system is subjected to certain external loads, such as aerodynamic and hydrodynamic forces, and instability occurs when the loads reach critical values. Because of pressure differences of fluids across the rotor disk, the aerodynamic and hydrodynamic loads exerted on a rotating shaft can be equivalent to the combination of an axial force, bending moments, and torques. Stability of beam-type structures subjected to these loads were discussed by Bolotin[3] and Ziegler[4] using the Euler method, and by Barsoum and Gallagher[5] using the finite element method in a static approach.

In the past few decades, various mathematical methods had been developed to investigate the dynamics of rotor systems. A comprehensive review paper of these methods was made in a recent work by Eshleman.[6] With the improvements of computer's hardware and software, finite element methods have become the most popular application techniques in analyses of complicated structures. Ruhl[7] first used the finite element method to study a rotating shaft, but some important effects such as the rotatory inertia, gyroscopic moments, and shear deformations were not included in his model. Subsequently, Dimaragonas,[8] Nelson and MacVaugh,[9] and Nelson[10] proposed modified finite element models to include some effects that were not taken into account in Ruhl's work. In the above-mentioned finite element models, in addition to contributions of the translational inertia and bending stiffness, the effects of the rotatory inertia, gyroscopic moments, shear deformations, axial loads, axial torques, and internal damping can be successfully taken into account. In addition, Chen and Ku[11,12] effectively utilized Nelson's model[10] to investigate the dynamic stability of a shaft-disk system subjected to an axial periodic force.

In the present work, the variation of natural whirl speeds and instability of a rotating shaft subjected to an axial compressive load, moments, and torques are studied in a kinetic approach. To obtain discrete equations of motion of the system and to acquire accurate numerical results, a finite element model of a Timoshenko beam proposed by Thomas and Abbas[13] is adopted. This model is successfully used to investigate vibration problems of rotating blades in Refs. 14 and 15. By using the model, all kinds of boundary conditions of beam-type structures can be satisfied, and only a few elements are needed to obtain good results.

Received June 12, 1993; revision received Sept. 20, 1994; accepted for publication Dec. 14, 1994.

*Professor, Department of Mechanical Engineering.
†Graduate Student, Department of Mechanical Engineering.

II. Finite Element Formulation

Energy of the Shaft

A cantilever rotating shaft with a rigid disk at its end and a fixed reference XYZ: $\mathcal{F}$ triad, with the X axis being coincident with the undeformed rotor centerline, is illustrated in Fig. 1. In a deformed state, an element of the shaft of length dx, located at a distance x from the left end, can be described by the translations $V(x,t)$ and $W(x,t)$ of the center of the element in the Y and Z directions, as well as the small rotations $\phi_y(x,t)$ and $\phi_z(x,t)$ and the twisting angle $\beta(x,t)$ about Y, Z, and X. For a circular shaft, the kinetic energy KE_s and the strain energy U_s, taking account of the effects of the gyroscopic moments, rotatory inertia, and shears, are given by

$$KE_s = \frac{1}{2}\int_L \left[\rho A\dot{V}^2 + \rho A\dot{W}^2 + \rho I_P(\dot{\theta}+\dot{\beta})^2 + \rho I\dot{\phi}_y^2 + \rho I\dot{\phi}_z^2 + 2\rho I_P\dot{\theta}\dot{\phi}_y\phi_z\right]dx \tag{1}$$

$$U_s = \frac{1}{2}\int_v \sigma_{ij}\cdot\varepsilon_{ij}\,dv = \frac{1}{2}\int_L \left[kGA(V'-\phi_z)^2 + kGA(W'+\phi_y)^2 + EI\phi_y'^2 + EI\phi_z'^2 + GI_P\beta'^2\right]dx \tag{2}$$

where an overdot denotes differentiation with respect to time t; ρ is the mass density of the material, A the cross-sectional area, I the area moments of inertia, I_P area polar moment of inertia, k the shear correction factor, G the shear modulus, and E Young's modulus. The prime indicates differentiation with respect to spatial coordinate x.

Kinetic Energy of Disk

The disk is regarded as a rigid body, and the kinetic energy can be calculated by integrating Eq. (1) over a finite length of the width of

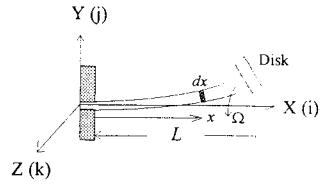

Fig. 1 Cantilever rotor system.

the disk and the deflections, V, W, β, ϕ_y, and ϕ_z are assumed to be independent of x. The kinetic energy of the disk can be expressed as

$$KE_d = \tfrac{1}{2}\big[m_d\dot{V}^2 + m_d\dot{W}^2 + J_P(\dot{\theta}+\dot{\beta})^2 + J\dot{\phi}_y^2 + J\dot{\phi}_z^2 + 2J_P\dot{\theta}\dot{\phi}_y\phi_z\big] \tag{3}$$

where m_d is the mass, J the mass moment of inertia, and J_P the polar mass moment of inertia of the disk.

Potential Energy due to End Loads

Stability of the rotating shaft subjected to four kinds of conservative loads at its end are studied in this work. The potential energies resulting from deformations of the shaft were evaluated by Ziegler[16] and Barsoum and Gallagher[5] and are listed as follows.

1) Axial compressive force P (Fig. 2a),

$$V_P = \frac{1}{2}P\int_L [V'^2 + W'^2]\,dx \tag{4}$$

2) Semitangential torque T_s (Fig. 2b),

$$V_{T_s} = \frac{1}{2}T_s\int_L [V'W'' - W'V'']\,dx \tag{5}$$

3) Quasitangential torque T_q (Fig. 2c),

$$V_{T_q} = \frac{1}{2}T_q\int_L [V'W'' - W'V'']\,dx + \frac{1}{2}T_qV'(L)W'(L) \tag{6}$$

4) Conservative moment M (Fig. 2d),

$$V_M = -M\int_L V''\beta\,dx \tag{7}$$

Finite Element Model

In the approximate of the Timoshenko beam, a number of different finite element models can be chosen.[17] In this paper, the finite element model proposed by Thomas and Abbas[13] is chosen to simulate the shaft. To derive discrete equations of motion of the system, the shaft is divided into N elements of equal length ℓ (as shown in Fig. 3), and the following expressions are introduced to nondimensionalize the deflections $V(x,t)$ and $W(x,t)$ and the spatial coordinate x.

$$V = \psi_y\ell, \qquad W = \psi_z\ell, \qquad x = (i-1)\ell + \ell\eta \tag{8}$$

The continuous functions ψ_y, ψ_z, ϕ_y, ϕ_z, and β in the domain of the element i are approximated by the combination of shape functions f_i and nodal coordinates $\{\zeta(t)\}_i$. The relationships are written in matrix expressions as

$$\begin{Bmatrix}\psi_y\\ \psi_z\\ \phi_y\\ \phi_z\\ \beta\end{Bmatrix} = \begin{bmatrix}\psi_{y,i} & \psi'_{y,i} & \psi_{y,i+1} & \psi'_{y,i+1}\\ \psi_{z,i} & \psi'_{z,i} & \psi_{z,i+1} & \psi'_{z,i+1}\\ \phi_{y,i} & \phi'_{y,i} & \phi_{y,i+1} & \phi'_{y,i+1}\\ \phi_{z,i} & \phi'_{z,i} & \phi_{z,i+1} & \phi'_{z,i+1}\\ \beta_i & \beta'_i & \beta_{i+1} & \beta'_{i+1}\end{bmatrix}\begin{Bmatrix}f_1(\eta)\\ f_2(\eta)\\ f_3(\eta)\\ f_4(\eta)\end{Bmatrix} \tag{9}$$

where

$$\{\zeta(t)\}_i = \begin{Bmatrix}\zeta_L\\ \zeta_R\end{Bmatrix}_i$$

$$\{\zeta_L\}_i = \{\psi_{y,i}\quad \psi'_{y,i}\quad \phi_{y,i}\quad \phi'_{y,i}\quad \psi_{z,i}\quad \psi'_{z,i}\quad \phi_{z,i}\quad \phi'_{z,i}\quad \beta_i\quad \beta'_i\}^T$$

$$\{\zeta_R\}_i = \{\psi_{y,i+1}\quad \psi'_{y,i+1}\quad \phi_{y,i+1}\quad \phi'_{y,i+1}\quad \psi_{z,i+1}\quad \psi'_{z,i+1}\quad \phi_{z,i+1}\quad \phi'_{z,i+1}\quad \beta_{i+1}\quad \beta'_{i+1}\}^T$$

$$f_1 = 1 - 3\eta^2 + 2\eta^3, \qquad f_2 = \eta - 2\eta^2 + \eta^3$$

$$f_3 = 3\eta^2 - 2\eta^3, \qquad f_4 = -\eta^2 + \eta^3$$

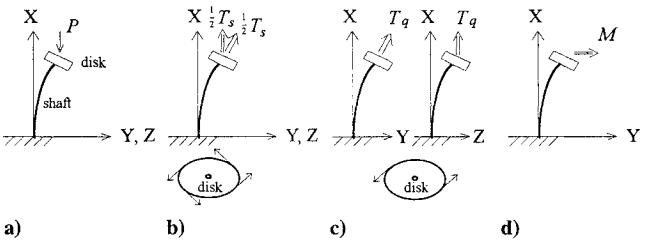

Fig. 2 Rotating shaft subjected to an end load.

Fig. 3 Divided shaft.

Upon substituting expressions (8) and (9) into Eqs. (1–7) and assembling results for all the elements and the disk, the kinetic energy, strain energy, and external works can be expressed in terms of the nodal displacement vector as

$$KE = KE_s + KE_d = \tfrac{1}{2}\{\dot{q}(t)\}^T[M]\{\dot{q}(t)\} + \{q(t)\}^T[\bar{G}]\{\dot{q}(t)\}$$
$$U = U_s = \tfrac{1}{2}\{q(t)\}^T[\bar{K}]\{q(t)\}$$
$$\bar{V} = \tfrac{1}{2}\{q(t)\}^T\big(P[K_g]_P + T_s[K_g]_{T_s} + T_q[K_g]_{T_q} - M[K_g]_M\big)\{q(t)\} \tag{10}$$

respectively, where $[M]$ is the mass matrix, $[\bar{G}]$ the gyroscopic matrix, and $[\bar{K}]$ the elastic stiffness matrix. $[K_g]_P$, $[K_g]_{T_s}$, $[K_g]_{T_q}$, and $[K_g]_M$ are geometric stiffness matrices due to the contributions of external loads, the axial compressive force, semitangential torque, quasitangential torque, and end moment, respectively.

Substituting Eq. (10) into the Hamilton's principle,

$$\delta\int_0^t (KE - U + \bar{V})\,dt = 0 \tag{11}$$

one obtains the global finite element equations as

$$[M]\{\ddot{q}\} + [G]\{\dot{q}\} + [K]\{q\} = 0 \tag{12a}$$

in which

$$[K] = \big([\bar{K}] - P[K_g]_P - T_s[K_g]_{T_s} - T_q[K_g]_{T_q} + M[K_g]_M\big) \tag{12b}$$

$$[G] = ([\bar{G}]^T - [\bar{G}]) \tag{12c}$$

To obtain solutions of the homogeneous Eqs. (12a), the equations are converted to an equivalent set of first-order ordinary differential equations known as Hamilton's canonical equations,

$$[M^*]\{\dot{p}(t)\} + [K^*]\{p(t)\} = 0 \tag{13}$$

where

$$\{p(t)\} = \begin{Bmatrix}\{\dot{q}(t)\}\\ \{q(t)\}\end{Bmatrix}, \qquad [M^*] = \begin{bmatrix}[0] & [M]\\ [M] & [G]\end{bmatrix}$$
$$[K^*] = \begin{bmatrix}-[M] & [0]\\ [0] & [K]\end{bmatrix} \tag{14}$$

and a solution of the governing equations is sought in the form $\{p(t)\} = e^{\lambda t}\{\Phi\}$, where $\lambda = \alpha + i\omega$. Finally, the eigenequations are obtained as follows:

$$\lambda[M^*]\{\Phi\} + [K^*]\{\Phi\} = 0 \tag{15}$$

in which ω is the natural whirl speed of the rotor system. If one of the real parts (α) of the eigenvalues (λ) is greater than zero, one of two possible types of instability will happen. When the associated natural whirl speed is zero, the divergent type of system instability occurs; flutter occurs if the whirl speed is greater than zero.

Table 1 Lateral frequency parameter $\lambda_\omega = \omega^2 \rho A L^4/EI$ for static shaft with various end conditions, $\Omega = 0$, N = number of finite elements, and r = radius of shaft

	Fixed free				Fixed fixed			
	Present			Ref.	Present			Ref.
$2L/r$	$N=2$	$N=3$	$N=4$	18	$N=2$	$N=4$	$N=8$	18
10	10.496	10.494	10.494	10.45	199.39	198.87	198.85	199.4
25	12.022	12.014	12.013	12.00	405.89	401.18	400.99	400.7
50	12.293	12.275	12.273	12.27	482.07	471.73	471.11	470.7
100	12.372	12.344	12.341	12.34	507.48	493.99	492.88	492.7
500	12.403	12.368	12.363	12.36	516.53	501.86	500.34	500.3
Slender shaft				12.36				500.5

III. Numerical Results and Discussion

The following nondimensional parameters and dimensions of the system are defined and used in the present results:

λ_ω = frequency parameter, $\omega^2(\rho AL^4/EI)$
$\bar{\omega}$ = whirl speed parameter, $\omega(\rho AL^4/EI)^{1/2}$
$\bar{\alpha}$ = exponential increment parameter, $\alpha(\rho AL^4/EI)^{1/2}$
δ = logarithmic decrement, $-2\pi\alpha/\omega$
R = slenderness parameter, $r/2L$, where r is the radius of shaft
$P(L^2/EI)$ = axial force factor
k_s = semitangential torque factor, $T_s L/(\pi EI)$
k_q = quasitangential torque factor, $T_q L/(\pi EI)$
k_M = end conservative moment factor, $ML/(\pi^2 EIGI_P)^{1/2}$
Ω = spin speed of the shaft, $\dot{\theta}$

Dimensions of the rotor system are given as follows:

$$E = 207\text{E}+9\ \text{N/m}^2 \qquad G = 79.6\text{E}+9\ \text{N/m}^2 \qquad \nu = 0.3$$

$$k = 0.89 \qquad r = 0.04\ \text{m} \qquad L = 0.5\ \text{m}$$

$$m_d = 7.5\ \text{kg} \qquad J = 0.019\ \text{kg-m} \qquad J_P = 0.0369\ \text{kg-m}$$

$$\rho = 7680\ \text{kg/m}^3$$

To evaluate the accuracy of the present finite element model and the program we developed, the frequency parameter of a static shaft with various end conditions and the whirl speed parameter of a rotating Rayleigh beam are studied and are compared with the published works of Refs. 18 and 19, respectively. As is shown in Tables 1 and 2, the convergence test is well made and the accuracy of the present finite element model is quite satisfactory. The variations of the critical load factors of the static shaft with the slenderness parameter are plotted in Fig. 4. As the shaft becomes slender, the critical load factors increase and asymptotically approach the convergent values which are Ziegler's solutions[4] obtained by the static approach for the Euler–Bernoulli beam.

In the following computations, the shaft is modeled as an assembly of four finite elements of equal length. As can be seen from Tables 1 and 2, the four-element model is sufficient to obtain accurate numerical results for the analyses of a cantilever rotor system. To study the effects of axial compressive force on dynamic characteristics of the rotor system, the variation of whirl speed parameters $\bar{\omega}$ of the rotating shaft vs the axial force are plotted in Fig. 5. Here, only the contribution of P is retained in Eq. (12b), and three cases with different spin speeds are studied. It is found from Fig. 5 that the speeds of the most important whirling modes 1B and 1F (the first backward and first forward modes) of the system all decrease obviously as the axial force factor increases. In the operations, a rotor system may be excited to whirl in the backward mode in specific situations or in the forward mode in other situations. When the axial compressive force is one of the major external loads of the system, it is necessary to take account of effects of the axial force to predict accurately the natural whirling speeds for all operating situations because the effects on both modes (as shown in Fig. 5) are significant. In addition to the variation of whirl speeds with external loads,

Table 2 Comparison of the present whirl speed parameter $\bar{\omega} = \omega(\rho AL^4/EI)^{1/2}$ to the results of the Ref. 19 for a rotating Rayleigh beam with hinged-hinged end conditions, spin speed: $\Omega = 3000$ rad/s, B = backward mode, and F = forward mode

	1B	1F	2B	2F
Ref. 19[a]	9.695	9.986	38.43	39.58
Present[b]	9.723	10.01	38.87	40.05

[a]Distributed transfer function method. [b]Finite element method.

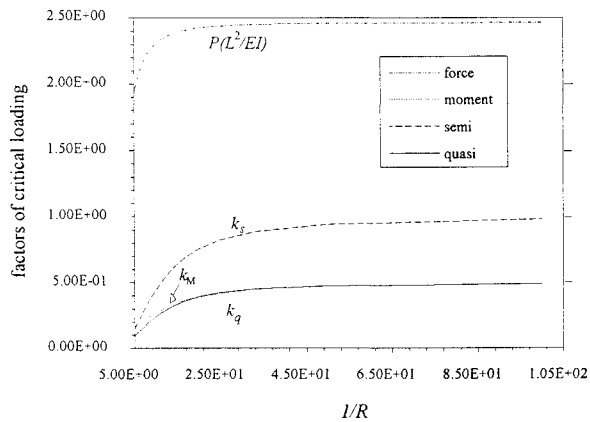

Fig. 4 Variation of the factors of critical loads vs slenderness parameter R.

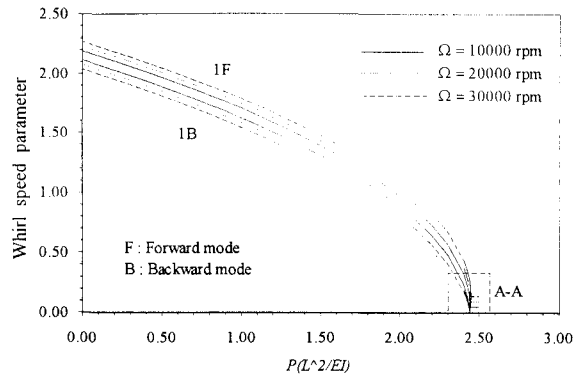

Fig. 5 Variation of whirl speed parameter $\bar{\omega}$ vs axial force factor, R = 0.04.

the type of system instability is also interesting to us. When the force factor is close to the buckling value (2.439) of the static shaft, the first backward whirl speeds with different spin speeds all approach zero; i.e., this phenomenon is independent of spin speeds (see the details in inset A-A in Fig. 6). As the load factor slightly and continuously increases, the first backward modes in the three cases all disappear and become new forward modes. At this moment, the first and second whirling modes of the system are all forward, and the two associated whirl speed parameters would be close to each other very quickly. Finally, when the force factor is equal to a critical

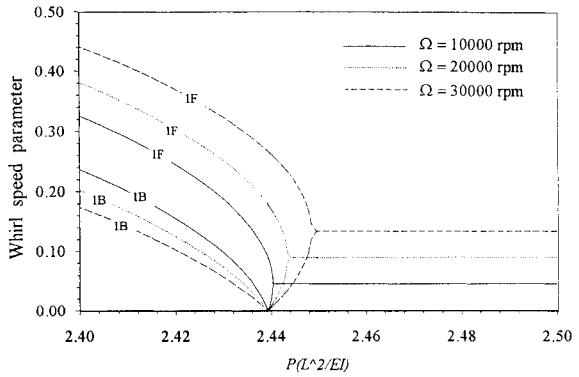

Fig. 6 Details of inset A-A in Fig. 5.

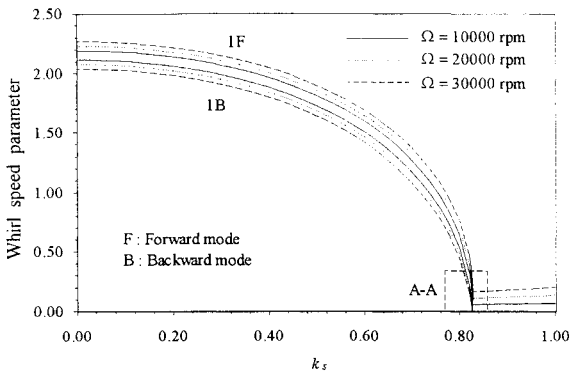

Fig. 7 Variation of whirl speed parameter $\bar{\omega}$ vs semitangential torque factor, R = 0.04.

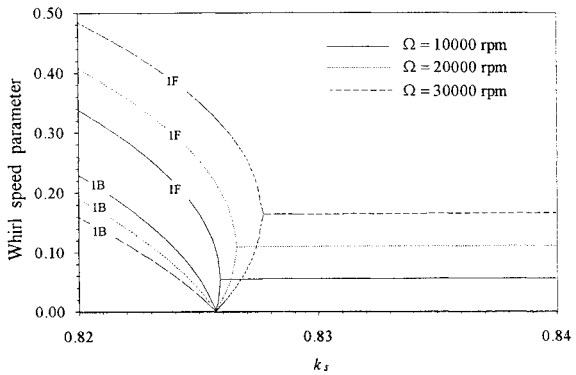

Fig. 8 Details of inset A-A in Fig. 7.

value (they are 2.440, 2.444, and 2.450 in the cases with 10,000, 20,000, and 30,000 rpm, respectively), the speeds of the two lowest modes are equal, and one of their associated logarithmic decrements δ decreases as the force factor increases continuously. Henceforth, the flutter occurs. We can also find from Figs. 6 and 11 that the critical force factors in the cases with high-spin speeds are greater than those in the cases with low-spin speed; that is, gyroscopic effects make the shaft more stable when the system is subjected to axial compressive forces. A similar phenomenon can be observed in Figs.7 and 8 when the rotating shaft is subjected to the semitangential torque. This is a special phenomenon for a rotating shaft and the phenomenon is not observed in analyses of the beam and the rotor system neglecting gyroscopic effects, where the type of system instability is divergence.

The influences of the quasitangential torque on natural whirl speeds of the system (as shown in Fig. 9) are quite different from those of the loads already mentioned. As the torque factor k_q increases, the whirl speeds of the first backward modes in the three cases all decrease and become zero when the load factor reaches the same critical value (0.425). Later, the speeds of the 1Bs will be always zero and the associated exponential increments $\bar{\alpha}$ become nonzero (see Fig. 12) when the loading factor increases continuously. The divergent type of system instability occurs at the same critical torque factor in the three cases with different spin speeds. Also, we can find that the natural whirl speeds of the first forward modes slightly increase, and all the speeds move closer gradually as the loading factor increases. This trend is not observed in the analyses of the beam in which all natural frequencies decrease as the load increases.

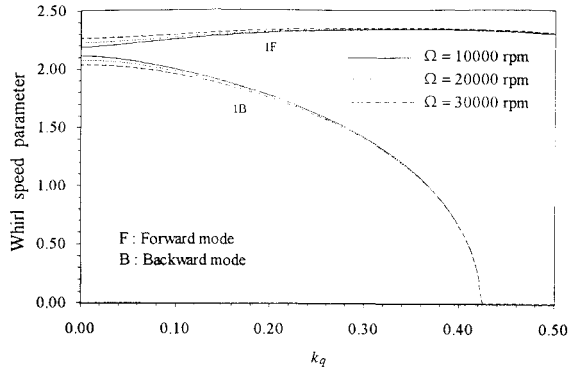

Fig. 9 Variation of whirl speed parameter $\bar{\omega}$ vs quasitangential torque factor, R = 0.04.

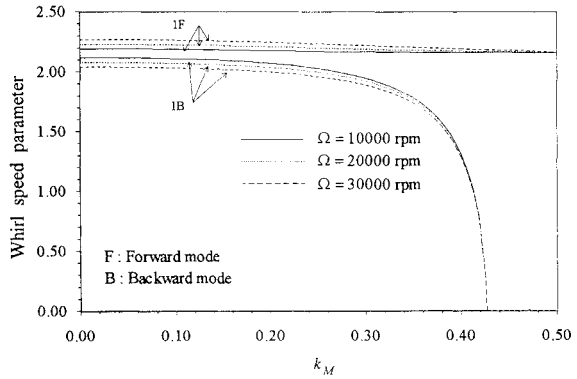

Fig. 10 Variation of whirl speed parameter $\bar{\omega}$ vs moment factor, R = 0.04.

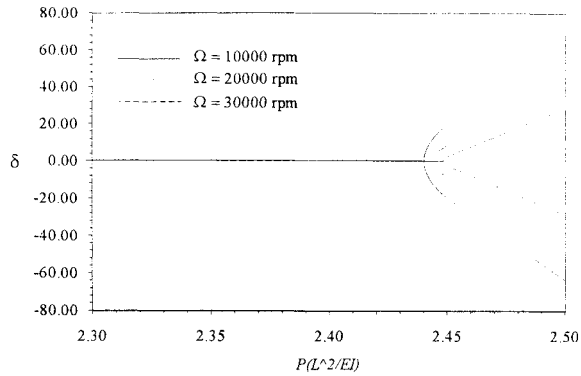

Fig. 11 Associated logarithmic decrement δ of the modes in Fig. 5.

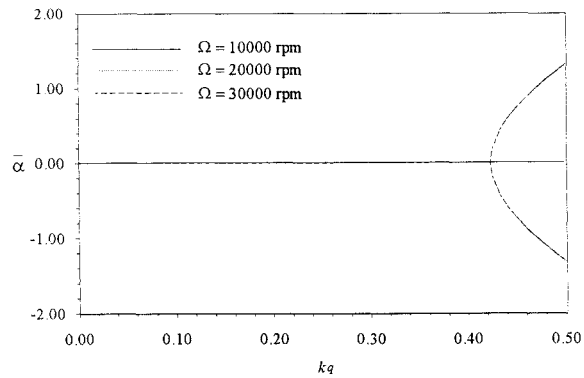

Fig. 12 Associated exponential increment parameter $\bar{\alpha}$ of the modes in Fig. 9.

The natural whirl speeds of the first backward and forward modes all decrease, but the trend is slight when the end moment factor is located in the small value range (see Fig. 10). When the loading factor is near the critical value (0.427), the whirl speeds of the backward modes in the three cases decrease sharply and approach zero quickly. Instability of the shaft subjected to such an end load is the same as that of the shaft subjected to the quasitangential torque, and the gyroscopic moments have no effects on the value of the critical load.

IV. Conclusion

The variation of whirl speeds and instability of a cantilever rotating shaft with a disk, subjected to four kinds of external loads, are studied in this paper. The finite element method is adopted to obtain numerical results. From the results presented here, it is found that natural whirl speeds of the shaft do not always decrease when the external loads increase but do increase when the system is subjected to the quasitangential torque. Two different types of system instability are observed when the loads reach the critical values. In the loading situations of the axial compressive force and semitangential torque, the type is flutter and gyroscopic effects make the system more stable. In the other two loading cases, the divergence occurs and the critical loads are not influenced by gyroscopic moments. This is an interesting phenomenon for a rotating shaft.

References

[1]Rankine, W. J. M., "On the Centrifugal Force of Rotating Shafts," *Engineer*, Vol. 27, 1869, p. 249.

[2]Vance, J. M., *Rotordynamics of Turbomachinery*, Wiley, New York, 1988.

[3]Bolotin, V. V., *Nonconservative Problems of the Theory of Elastic Stability*, Pergamon, New York, 1963.

[4]Ziegler, H., *Principles of Structural Stability*, Birkhauser, Basel, Switzerland, 1977.

[5]Barsoum, R. S., and Gallagher, R. H., "Finite Element Analysis of Torsional and Torsional-Flexural Stability Problems," *International Journal for Numerical Methods in Engineering*, Vol. 2, 1970, pp. 335–352.

[6]Eshleman, R. L., "Critical Speeds and Response of Flexible Rotor Systems," *Flexible Rotor-Bearing System Dynamics*, Vol. 1, American Society of Mechanical Engineers, New York, 1972.

[7]Ruhl, R. L., "Dynamics of Distributed Parameter Rotor Systems: Transfer Matrix and Finite Element Techniques," Ph.D. Dissertation, Cornell Univ., Ithaca, NY, 1970.

[8]Dimaragonas, A. D., "A General Method for Stability Analysis of Rotating Shafts," *Ingenieur-Archive 44*, Vol. 1, 1975, pp. 9–20.

[9]Nelson, H. D., and McVaugh, J. M., "The Dynamics of Rotor-Bearing Systems Using Finite Elements," *Journal of Engineering for Industry*, Vol. 98, No. 2, 1976, pp. 593–600.

[10]Nelson, H. D., "A Finite Rotating Shaft Element Using Timoshenko Beam Theory," *Journal of Mechanical Design*, Vol. 102, 1980, pp. 793–803.

[11]Chen, L. W., and Ku, D. M., "Dynamic Stability Analysis of a Rotating Shaft by the Finite Element Method," *Journal of Sound and Vibration*, Vol. 143, No. 1, 1990, pp. 143–151.

[12]Chen, L. W., and Ku, D. M., "Dynamic Stability of a Cantilever Shaft-Disk System," *Journal of Vibration and Acoustics*, Vol. 114, July 1992, pp. 326–329.

[13]Thomas, J., and Abbas, B. A. H., "Finite Element Model for Dynamic Analysis of Timoshenko Beam," *Journal of Sound and Vibration*, Vol. 41, 1975, pp. 291–299.

[14]Abbas, B. A. H., "Simple Finite Elements for Dynamic Analysis of Thick Pre-twisted Blades," *Aeronautical Journal*, 1979, pp. 450–453.

[15]Chen, L. W., and Chen, H. K., "The Vibrations of Pre-twisted Rotating Beams of General Orthotropy," *Journal of Sound and Vibration*, Vol. 167, 1993, pp. 529–539.

[16]Ziegler, H., "Stabilitätsprobleme bei geraden Stäben und Wellen," *ZAMP*, Vol. 2, 1951, pp. 265–292.

[17]Thomas, D. L., Wilson, J. M., and Wilson, R. R., "Timoshenko Beam Finite Elements," *Journal of Sound and Vibration*, Vol. 31, 1973, pp. 315–330.

[18]Shastry, B. P., and Rao, G. V., "Dynamic Stability of Bars Considering Shear Deformation and Rotatory Inertia," *Computers and Structures*, Vol. 19, 1984, pp. 823–827.

[19]Kuang, W., and Tan, C. A., "Vibration of a Rotating Stepped Beam by the Distributed Transfer Function Method," *Vibration of Rotating Systems*, DE-Vol. 60, American Society of Mechanical Engineers, New York, 1993, pp. 219–227.